International Symposium
On Turbulence and Shear Flow
Phenomena (TSFP-8)
August 28 - 30, 2013 Poitiers, France

MODELING OF TURBULENCE EFFECT ON RADAR REFLECTIVITY FACTOR IN CLOUDS

Keigo MATSUDA[1], Ryo ONISHI[1], Masaaki HIRAHARA[2], Keiko TAKAHASHI[1],

Ryoichi KUROSE[2], and Satoru KOMORI[2]

[1]Earth Simulator Center
Japan Agency for Marine-Earth Science and Technology (JAMSTEC)
3173-25 Showa-machi, Kanazawa-ku, Yokohama, Kanagawa 236-0001, Japan
k.matsuda@jamstec.go.jp onishi.ryo@jamstec.go.jp takahasi@jamstec.go.jp

[2]Department of Mechanical Engineering and Science
Advanced Research Institute of Fluid Science and Engineering
Kyoto University
Kyoto daigaku-Katsura, Nishikyo-ku, Kyoto 615-8540, Japan
hirahara.masaaki.85n@st.kyoto-u.ac.jp kurose@mech.kyoto-u.ac.jp komori@mech.kyoto-u.ac.jp

ABSTRACT

This study proposes a radar reflectivity factor model considering the effect of turbulent clustering of cloud droplets. A three-dimensional direct numerical simulation of particle-laden isotropic turbulence is conducted to obtain turbulent clustering data. The power spectrum of droplet number density fluctuation, on which the radar reflectivity factor depends, is calculated from the turbulent clustering data. The power spectrum shows strong dependency on the Stokes number. It is confirmed that the proposed model can predict the Stokes number and the wavenumber dependencies of the turbulent clustering effect.

INTRODUCTION

Clouds play crucial roles in the heat and water systems of the Earth. A large number of observations have been conducted to understand the cloud physics. The radar observation is one of the powerful tools since it can provide spatial distribution data regarding the cloud microphysical properties such as the cloud water mixing ratio and effective droplet radius (Okamoto *et al.*, 2007; Stephens *et al.*, 2008). In the radar observation, microwave is transmitted from an antenna toward a target cloud and the reflected microwave is received and analyzed. The relation between the transmitted power, P_t, and the received power, P_r, of the microwave is given as the following radar equation:

$$P_r = \frac{P_t G^2 k_m^2 |K|^2 V}{4^5 R^4} Z, \tag{1}$$

where G is the antenna gain, k_m the wavenumber of microwave, R the distance between the antenna and the cloud, K the dielectric coefficient of a water droplet, V the measurement volume and Z the radar reflectivity factor. An important point is that Z is dependent on the cloud microphysical properties. This means that the cloud properties can be estimated from Z under some assumptions: large-scale homogeneity and small-scale randomness of cloud droplet distribution are usually assumed. However, cloud turbulence generates nonuniform spatial distribution of droplets, which is referred to as turbulent clustering (Maxey, 1987; Chen *et al.*, 2006). This turbulent clustering obviously contradicts the randomness assumption for the analysis of Z. This may cause a significant observational error (Gossard & Strauch, 1983; Kostinski & Jameson, 2000; Dombrovsky & Zaichik, 2010). It is, therefore, of great importance to clarify the effect of turbulent clustering on Z. This study aims to develop a radar reflectivity factor model considering the effect of turbulent clustering based on the data from a three-dimensional direct numerical simulation (DNS) of particle-laden isotropic turbulence.

COMPUTATIONAL METHOD

Air Turbulence

Governing equations of the turbulent air flow are the continuity and Navier-Stokes equations for three-dimensional incompressible flows:

$$\frac{\partial u_i}{\partial x_i} = 0, \tag{2}$$

$$\frac{\partial u_i}{\partial t} + \frac{\partial u_i u_j}{\partial x_j} = -\frac{1}{\rho_g}\frac{\partial p}{\partial x_i} + \nu \frac{\partial^2 u_i}{\partial x_j \partial x_j} + F_i, \tag{3}$$

where u_i is the fluid velocity in i-th direction, ρ_g the air density, p the pressure, ν the kinematic viscosity and F_i the external force term. The fourth-order central difference scheme (Morinishi *et al.*, 1998) was used for the advection term, and the second-order Runge-Kutta scheme for time integration. The velocity and pressure were coupled by the HSMAC method (Hirt & Cook, 1972). Statistically steady turbulence was generated by applying the Reduced-Communication Forcing (RCF) (Onishi *et al.*, 2011), which maintains the intensity of large-scale eddies keeping high parallel efficiency, to the external force, F_i.

Droplet Motions

Droplet motions were tracked by the Lagrangian method. The governing equation of the motion is

$$\frac{dv_i}{dt} = -\frac{v_i - u_i}{\tau_p}, \tag{4}$$

where v_i is the droplet velocity and τ_p the droplet relaxation time. Droplets were assumed as Stokes particles, whose relaxation time, τ_p, is given as

$$\tau_p = \frac{\rho_p}{\rho_g}\frac{2r_p^2}{9\nu}, \tag{5}$$

where r_p is the droplet radius and ρ_p the water density. Effects of gravity and collisions between droplets were neglected for simplicity (Matsuda *et al.*, 2012).

Computational Conditions

The computational domain was set to a cube with length of $2\pi L_0$, where L_0 is the representative length. The periodic boundary conditions were applied in all three directions. The DNS was performed for the case where the Taylor-microscale-based Reynolds number, Re_λ ($= u' l_\lambda / \nu$, where u' is the RMS value of velocity fluctuation, l_λ the Taylor microscale), was 203. The number of grid points and the representative length scale were set to 512^3 and 0.04 m, respectively. The droplet radius, r_p, was varied so that the Stokes number, St ($= \tau_p/\tau_\eta$, where τ_η is the Kolmogorov time), became 0.05, 0.1, 0.2, 0.5, 1.0, 2.0 and 5.0.

RADAR REFLECTIVITY FACTOR

There have been several studies reporting that the radar reflectivity factor, Z, of nonuniformly-dispersed particles is larger than that of randomly-dispersed particles (Kostinski & Jameson, 2000; Erkelens *et al.*, 2001). The increment is attributed to the coherent microwave scattering, which involves an effect of interference between two microwaves scattered by different particles. In the case where droplets are randomly dispersed in atmosphere, the effect of interference is cancelled and becomes zero. Thus, the radar reflectivity factor, Z_{random}, of randomly-located monodispersed droplets is calculated from the sum of the Rayleigh scattering intensity by droplets in the measurement volume and given as follows:

$$Z_{\mathrm{random}} = 2^6 r_p^6 n_p, \tag{6}$$

where n_p is the droplet number density. On the other hand, in the case where droplets form clusters, the effect of interference appears as an additional term. That is, the radar reflectivity factor, Z_{cluster}, for monodispersed clustering droplets is given as follows (Gossard & Strauch, 1983; Kostinski & Jameson, 2000; Erkelens *et al.*, 2001):

$$Z_{\mathrm{cluster}} = Z_{\mathrm{random}} + \frac{2^7\pi^2 r_p^6}{\kappa^2} E_{np}(\kappa), \tag{7}$$

where κ is the absolute value of the difference between the incident and scattered wavenumber vectors, $\mathbf{k}_{\mathrm{inc}}$ and $\mathbf{k}_{\mathrm{sca}}$, respectively, and given as $\kappa = |\mathbf{k}_{\mathrm{inc}} - \mathbf{k}_{\mathrm{sca}}|$. In the case where the antenna receives backward scattering and the Doppler effect is small enough, κ becomes $2k_m$. $E_{np}(k)$ is the power spectrum of droplet number density fluctuation, which represents the effect of turbulent clustering.

Unfortunately, there has not been a widely accepted analytical model for $E_{np}(k)$ (Jeffery, 2000). Thus, in this study, $E_{np}(k)$ was calculated from the DNS data as

$$E_{np}(k) = \frac{1}{\Delta k}\sum_{k-\frac{1}{2}\Delta k \le |\mathbf{k}| \le k+\frac{1}{2}\Delta k} \widetilde{\Phi}(\mathbf{k}), \tag{8}$$

$$\widetilde{\Phi}(\mathbf{k}) = \frac{1}{L_0^3}\left\langle \widetilde{n_p}(\mathbf{k})\widetilde{n_p}(-\mathbf{k})\right\rangle, \tag{9}$$

where $\widetilde{\Phi}(\mathbf{k})$ is the spectral density function of droplet number density fluctuation and $\widetilde{n_p}(\mathbf{k})$ the Fourier coefficients of the spatial droplet number density distribution, $n_p(\mathbf{x})$. The bracket, $\langle\cdot\rangle$, represents the ensemble average. The continueus function of $n_p(\mathbf{x})$ is given as

$$n_p(\mathbf{x}) = \sum_{i=1}^{N_p}\delta(\mathbf{x} - \mathbf{x}_{p,i}), \tag{10}$$

where $\mathbf{x}_{p,i}$ is the position vector of the i-th droplet inside a target domain, N_p the total number of droplets, $\delta(\mathbf{x})$ the Dirac delta function. The Fourier coefficients of Eq. (10) are then given as

$$\widetilde{n_p}(\mathbf{k}) = \frac{1}{(2\pi)^3}\sum_{i=1}^{N_p}\exp(-\mathrm{i}\mathbf{k}\cdot\mathbf{x}_{p,i}). \tag{11}$$

Finally, substitution of Eq. (11) into Eq. (9) yields $\widetilde{\Phi}(\mathbf{k})$ as

$$\frac{\widetilde{\Phi}(\mathbf{k})}{\langle n_p\rangle^2 L_0^3} = \frac{1}{N_p^2}\left\langle \sum_{i=1}^{N_p}\exp\left(-\mathrm{i}\mathbf{k}\cdot\mathbf{x}_{p,i}\right)\sum_{j=1,j\neq i}^{N_p}\exp\left(\mathrm{i}\mathbf{k}\cdot\mathbf{x}_{p,j}\right)\right\rangle. \tag{12}$$

Eq. (12) is calculated for each discrete wavenumber vector, $\mathbf{k}$, which satisfies $\mathbf{k} = (m_1/L_0, m_2/L_0, m_3/L_0)$ for arbitral integer numbers; m_1, m_2 and m_3.

RESULTS AND DISCUSSION

Droplet Distribution in Turbulence

Figure 1 shows the distributions of droplets within the range of $0 < z < 4l_\eta$, where l_η is the Kolmogorov scale, for $St = 0.05$, 0.2, 1.0 and 5.0. Void areas due to turbulent

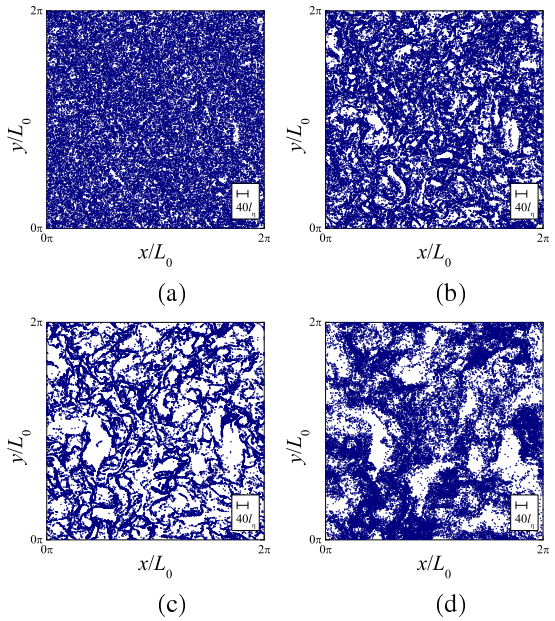

Figure 1. Spatial distributions of droplets obtained by DNS for (a) $St = 0.05$, (b) 0.2, (c) 1.0 and (d) 5.0. Droplets located within the range of $0 < z < 4l_\eta$ are drawn.

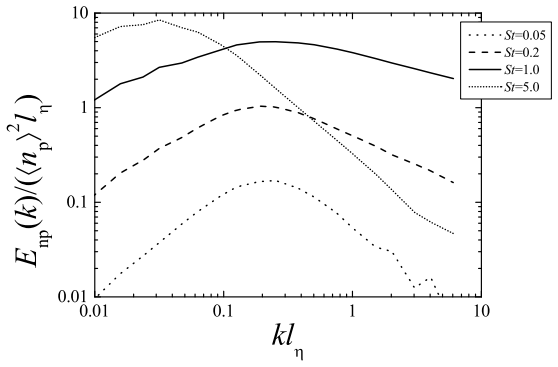

Figure 2. Power spectra of droplet number density fluctuation for $St = 0.05$, 0.2, 1.0 and 5.0 obtained from DNS data.

clustering are clearly observed for $St = 1.0$, and less clear for $St < 1$ or $St > 1$. It is also observed that small void areas, whose sizes are smaller than $10l_\eta$, for $St = 5.0$ are less frequent and less clear than those for $St = 1.0$.

Figure 2 shows $E_{np}(k)$, the power spectra of droplet number density fluctuation. The horizontal and vertical axes are normalized by the Kolmogorov scale, l_η, and the average number density, $\langle n_p \rangle$. It is clear that $E_{np}(k)$ strongly depends on St. For the cases of $St < 1$, the peak of $E_{np}(k)$ locates around $kl_\eta \sim 0.2$ and becomes larger as St becomes closer to 1. On the other hand, for the cases of $St > 1$, the peak location moves to lower wavenumber as St increases. These indicate that, for the $St < 1$ cases, the scale of the void area is almost constant but the number density difference between the void area and cluster increases as St increases. On the other hand, for the $St > 1$ cases, the scale of void area increases as St increases. These features are also observed in Figure 1. Another important point is that $E_{np}(k)$ does not show the monotonically-decreasing trend with $-5/3$ and -1 power laws, which are observed in the power spectrum of scalar concentration fluctuation. This is because the fluctuation of droplet number density is mainly generated in the energy-dissipative range of turbulence. This fact indicates that model functions for the well-known scalar concentration spectrum are not applicable to the turbulent clustering case.

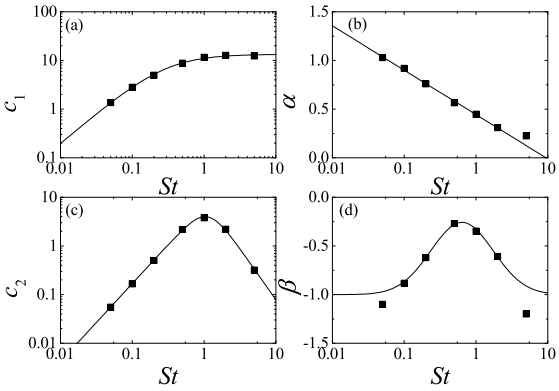

Figure 3. Model parameters in Eq. (13) versus the Stokes number, St: (a) c_1; (b) α; (c) c_2; (d) β. Solid lines show the present fittings.

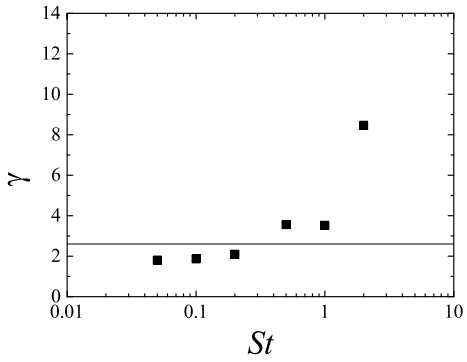

Figure 4. Model parameter, γ, in Eq. (13) versus the Stokes number, St. Solid line indicates the averaged value for $St \leq 1.0$.

Modeling of Turbulent Clustering Effect

A new empirical radar reflectivity factor model is developed as a function of kl_η and St by fitting curves to $E_{np}(k)$ in Figure 2. Here, we assumed that a power spectrum of number density fluctuation approaches asymptotically to $E_{np}(k) \approx c_1(kl_\eta)^\alpha$ and $E_{np}(k) \approx c_2(kl_\eta)^\beta$ in small and large wavenumber regions, respectively. Therefore, the model function of the spectrum, $E_{np,model}(k)$, was set as

$$\frac{E_{np,model}(k)}{\langle n_p \rangle^2 l_\eta} = \frac{c_1 (kl_\eta)^\alpha}{\left\{1 + \left[\frac{c_1}{c_2}(kl_\eta)^{(\alpha-\beta)}\right]^\gamma\right\}^{1/\gamma}}, \qquad (13)$$

where γ is the parameter for adjusting the peak value. Figure 3 shows the parameters, c_1, α, c_2 and β, for each of the Stokes numbers. The solid lines are the present fitting results. Note that the reference data for c_1 and α for $St = 5.0$ were fewer than those for the other St. Thus α for $St = 5.0$ was not used for the fitting. In addition, from the theoretical view point, β for $St \ll 1$ should be -1, which is the power index of the power spectrum of scalar con-

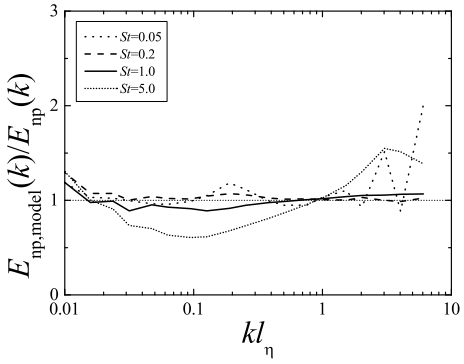

Figure 5. Ratio of the power spectrum obtained from the proposed model to that from DNS data.

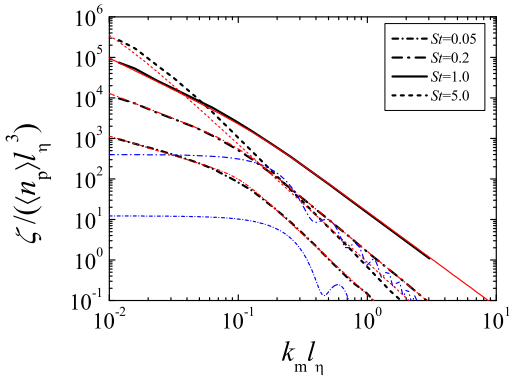

Figure 6. Clustering coefficient obtained from (red) the present model, (black) the reference $E_{np}(k)$ data in Figure 2, and (blue) Dombrovsky & Zaichik (2010), which is for only $St < 0.6$.

centration fluctuation in the viscous-convective range. On the other hand, β for $St \gg 1$ is unknown. This study assumed β approaches to -1 for $St \ll 1$ and $St \gg 1$. Figure 4 shows the parameter, γ, for Eq. (13). It is shown that γ is nearly constant for $St \leq 1.0$, while it becomes larger for $St > 1.0$. This study set γ to the average value for the range of $St \leq 1.0$, i.e., ignored the γ values for $St > 1.0$. Nevertheless, Figure 5, which shows the ratio of the predicted power spectrum, $E_{np,model}(k)$, to the reference power spectrum, $E_{np}(k)$, shows a good agreement between the predicted and reference spectra for all the St cases. All the ratios remain within the range from 0.5 to 2.0 for the whole wavenumber.

Comparison of Radar Reflectivity Factor Models

The radar reflectivity factor, Z, is estimated by Eq. (7) and $E_{np,model}(k)$, and compared with that calculated from the reference $E_{np}(k)$ data in Figure 2 and that estimated by Dombrovsky & Zaichik (2010). Dombrovsky & Zaichik (2010) evaluated the increment of Z due to turbulent clustering using following equations (Kostinski & Jameson, 2000):

$$Z_{cluster} = (1+\zeta) Z_{random}, \tag{14}$$

$$\zeta = \frac{4\pi \langle n_p \rangle}{\kappa} \int_0^\infty [g(r)-1] r \sin(\kappa r) dr, \tag{15}$$

where ζ is the clustering coefficient. $g(r)$ is the radial distribution function (RDF) defined as $g(r) = \langle n_p(\mathbf{x}) n_p(\mathbf{x}+\mathbf{r}) \rangle / \langle n_p \rangle^2$, where $r = |\mathbf{r}|$. Dombrovsky & Zaichik (2010) adopted a theoretical RDF model (Zaichik & Alipchenkov, 2007), which is applicable to the case of $St < 0.6$ and $Re_\lambda > 30$. Figure 6 shows the clustering coefficient, ζ. The horizontal axis is the wavenumber of microwave, k_m, normalized by l_η. The vertical axis is normalized by $\langle n_p \rangle l_\eta^3$ for eliminating the effect of droplet number density (Dombrovsky & Zaichik, 2010). ζ obtained from the reference $E_{np}(k)$ data shows a strong dependency on St and a monotonic decreasing trend against the nondimensional wavenumber $k_m l_\eta$. The St dependensy is also seen in Dombrovsky & Zaichik (2010). However, the monotonic decreasing trend is not seen: ζ of Dombrovsky & Zaichik (2010) is almost constant in the low wavenumber region and decreases with some oscillations as the wavenumber increases. This is because the theoretical RDF model, on which Dombrovsky & Zaichik (2010) based, assumes that the separation, r, is smaller than l_η, although Eq. (15) contains an integration of the RDF from 0 to infinity. In contrast, ζ obtained from the present model shows both the St dependency and the monotonic decreasing trend. These results confirm that the present radar reflectivity factor model can appropriately predict the turbulent clustering effect.

CONCLUSION

This study has proposed the radar reflectivity factor model considering the effect of turbulent clustering of cloud droplets. A three-dimensional direct numerical simulation (DNS) of particle-laden isotropic turbulence has been conducted to obtain turbulent clustering data. The power spectrum of droplet number density fluctuation has been calculated from the turbulent clustering data. The results show that the power spectrum strongly depends on the Stokes number. For the Stokes number smaller than 1, the peak of the power spectrum locates around 0.2 times of the Kolmogorov wavenumber and becomes higher as the Stokes number becomes closer to 1. On the other hand, for the Stokes number larger than 1, the peak location moves to lower wavenumber as the Stokes number increases. The present radar reflectivity factor model has been developed based on a sophisticated empirical fitting to the power spectrum in order to consider these trends. It has been confirmed that the model can predict the Stokes number dependency and the wavenumber dependency of the turbulent clustering effect.

REFERENCES

Chen, L., Goto, S. & Vassilicos, J.C. 2006 Turbulent clustering of stagnation points and inertial particles. *Journal of Fluid Mechanics* **553**, 143–154.

Dombrovsky, L.A. & Zaichik, L.I. 2010 An effect of turbulent clustering on scattering of microwave radiation by small particles in the atmosphere. *Journal of Quantitative Spectroscopy and Radiative Transfer* **111**, 234–242.

Erkelens, J.S., Venema, V.K.C., Russchenberg, H.W.J. & Ligthart, L.P. 2001 Coherent scattering of microwave by particles: Evidence from clouds and smoke. *Journal of Atmospheric Science* **58**, 1091–1102.

Gossard, E.E. & Strauch, R.G. 1983 *Radar Observation of*

Clear Air and Clouds, *Developments in Atmospheric Science*, vol. 14. New York: Elsevir.

Hirt, C.W. & Cook, J.L. 1972 Calculating three-dimensional flow around structures. *Journal of Computational Physics* **10**, 324–340.

Jeffery, C.A. 2000 Effect of particle inertia on the viscous-convective subrange. *Physical Review E* **61**, 6578–6585.

Kostinski, A.B. & Jameson, A.R. 2000 On the spatial distribution of cloud particles. *Journal of Atmospheric Science* **57**, 901–915.

Matsuda, K., Onishi, R., Kurose, R. & Komori, S. 2012 Turbulence effect on cloud radiation. *Physical Review Letters* **108**, 224502.

Maxey, M.R. 1987 The gravitational settling of aerosol particles in homogeneous turbulence and random flow fields. *Journal of Fluid Mechanics* **174**, 441–465.

Morinishi, Y., Lundm, T.S., Vasilyev, O.V. & Moin, P. 1998 Fully conservative higher order finite difference schemes for incompressible flow. *Journal of Computational Physics* **143**, 90–124.

Okamoto, H., Nishizawa, T., Takemura, T., Kumagai, H., Kuroiwa, H., Sugimoto, N., Matsui, I., Shimizu, A., Emori, S., Kamei, A. & Nakajima, T. 2007 Vertical cloud structure observed from shipborne radar and lidar: Mid-latitude case study during the mr01/k02 cruise of the research vessel mirai. *Journal of Geophysical Research* **112**, D08216.

Onishi, R., Baba, Y. & Takahashi, K. 2011 Large-scale forcing with less communication in finite-difference simulations of steady isotropic turbulence. *Journal of Computational Physics* **230**, 4088–4099.

Stephens, G.L., Vane, D.G., Tanelli, S., Im, E., Durden, S., Rokey, M., Reinke, D., Partain, P., Mace, G.G., Austin, R., L'Ecuyer, T. Haynes, J., Lebsock, M., Suzuki, K., Waliser, D., Wu, D., Kay, J., Gettelman, A., Wang, Z. & Marchand, R. 2008 Cloudsat mission: Performance and early science after the first year of operation. *Journal of Geophysical Research* **113**, D00A18.

Zaichik, L.I. & Alipchenkov, V.M. 2007 Refinement of the probability density function model for preferential concentration of aerosol particles in isotropic turbulence. *Physics of Fluids* **19**, 113308.